Journal of Materials Chemistry B

Accepted Manuscript

ROYAL SOCIETY OF CHEMISTRY

www.rsc.org/materialsB

Cite this: DOI: 10.1039/x0xx00000x

Supplementing π-Systems: Eumelanin and Graphene-Like Integration Towards High Conductive Material for Mammalian Cell Culture Bio-interface.

Received ooth January 2012,
Accepted ooth January 2012

DOI: 10.1039/x0xx00000x

www.rsc.org/

Valentina Gargiulo,[a] Michela Alfè,[a]Roberto Di Capua,[b,c]Anna Rita Togna,[d] Vittoria Cammisotto,[d]Silvana Fiorito,[e]Anna Musto,[f,g] Angelica Navarra,[f,g] Silvia Parisi,[f,g] and Alessandro Pezzella,[h*]

Abstract. Organic (bio)electronics appears the first target for a competitive exploitation in material science of eumelanins, the black insoluble photoprotective human biopolymers. Nonetheless, the low conductivity of these pigments is limiting the implementation of eumelanin-based devices. Here we present a novel organic/organic hybrid material (EUGL) by integration of conductive Graphene-Like (GL) layers within EUmelanin pigment (EU). GL layers were obtained by a two-step oxidation/reduction of carbon black. The stability of GL over a wide pH range and the self-assembling tendency place this material in a leading position for the fabrication of hybrid materials in aqueous media. EUGL was obtained inducing the polymerization of eumelanin precursors (5,6-dihydroxyindole, DHI and 5,6-dihydroxyindole-2 carboxylic acid, DHICA) in water media containing GL layers. The new material featured promising biocompatibility and an increased conductivity with respect to eumelanin by four orders of magnitude.

Introduction

Organic (bio)electronics[1,2] scope is largely dictated by the chemical nature of the materials that transduce signals across the biotic/abiotic interface. Among materials under investigation as candidates for functional biocompatible interfaces, the human pigment eumelanin is currently gaining increasing interest.[3-6]This black insoluble and heterogeneous pigment of human skin, hair, eyes and nigral neurons (neuromelanin)[7, 8] arises biogenetically from the aminoacid tyrosine via the oxidative polymerization of 5,6-dihydroxyindole (DHI) and/or 5,6-dihydroxyindole-2-carboxylic acid (DHICA).[5]A distinctive trait of eumelanin(s) is their unique assortment of chemical physical properties[3] including: (a) a broadband optical absorption in the UV-visible range;[9, 10](b) efficient UV-dissipative mechanisms;[11](c) photoconductivity in the solid state;[12](d) electronic-ionic hybrid conducting properties;[13, 14](e) hydration-dependent free radical properties;[15](f) metal ion-binding properties.[16] From structural point of view eumelanins appear as complicated disordered mixtures of different oligomeric and polymeric species arising by oxidative polymerization of the two indoles DHI and DHICA.[5] Nonetheless, a series of studies[5]have proved DHI-eumelanin[5] prepared by oxidation of the indole under biomimetic conditions, can efficiently acts as a model of the natural pigment.[17] Key elements characterizing the DHI polymerization and the arising eumelanin can be summarized as follows: (a)DHI polymers grow mainly via monomer−polymer or low oligomer−polymer coupling steps, rather than by large oligomer-oligomer interactions and the maximum aggregates apparent size attainable before precipitation is ca. 1200 nm;[18](b) the visible chromophore development associated with polymer growth, reflects a dual component, an intrinsic one, and an extrinsic dynamic one;[9, 10](c)the fundamental aggregates look like 2-D planar sheets[18](Figure 1).

Both chemical physical properties and structural features are the base of the interest toward this pigment,[4] however two main obstacles hampered a full exploitation of eumelanin based devices: (i)the eumelanin actual insolubility in any solvents,[3] preventing easy processability of the pigment as well as devices fabrication; (ii) it low conductivity,[15] limiting both the range of possible working potential and functional applications.

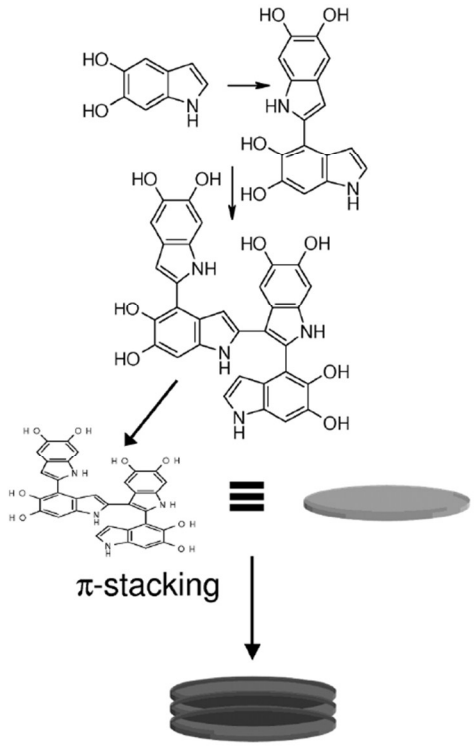

Figure 1. Schematic outline of eumelanin buildup.

On the other hand, the eumelanin biocompatibility[19-21]makes this material a candidate leading choice in a series of applicationsincluding: (a) functional interfaces connecting biological systems to electrical devices,[4, 22](b)devices translating optical and electronic stimuli into bio-signals for engineering functional biological tissues,[23](c) devices for advanced cell culture systems and single-cell managing,[24](d) devices for cell sorting and differentiation.[25]

In this scenario,a number of studies have recently appeared addressing eumelanin based functional devices[14, 26,27] as well as eumelanin films for nerve tissue engineering[23] and nonwoven fibers for cardiac tissue engineering.[19]

In a systematic investigation some of usaddressed the issue of eumelanin processability focusing on thin film fabrication with the main goal of obtaining both a complete chemical-structural control of the material and high quality film morphology. The combined use of biomimetic DHI oxidative polymerization and soft deposition techniques a such as MAPLE (Matrix Assisted Pulsed Laser Evaporation) allowed to gain the first objective[28, 29] while the design and developing of ad hoc solid state protocol for DHI oxidative polymerization (Ammonia Induced Solid State Polymerization, AISSP) allowed to obtain high quality easy accessible biocompatible eumelanin thin films.[30]

Although eumelanin films by AISSP protocol did show water depending charge transport attitude,[14, 30]the electrical properties of these films still settle far from the standards required in organic (bio)electronics.

Among the different strategies under investigation to improve electrical performance of eumelanin thin films, a clear-cut approach lies in hybridization with suitable conductive counterpart.

Delocalized electrons of π -conjugated molecules offer conductive pathway along their skeleton, attracting a great interest in the production of organic nanodevices.[31, 32] Numerous reports addressing the use of carbon nanotubes, reduced graphite oxide, graphene and graphene-like thin films as ideal transparent electrodes for optoelectronic devices have been presented in the past years [33, 3435]

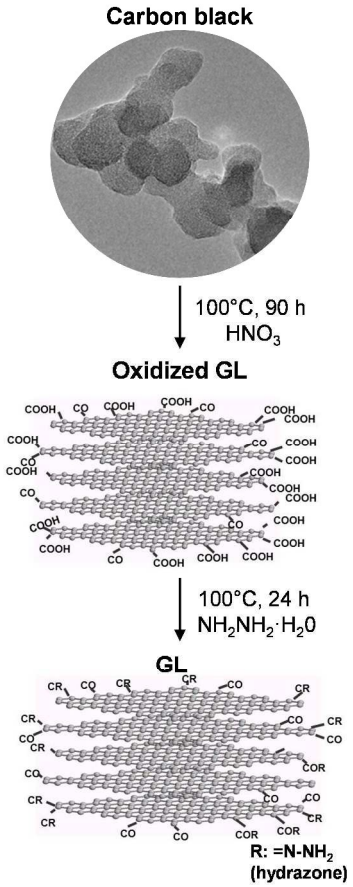

Figure 2. Synthetic pathway and representation of the hypothesized morphologies of GL layers.

In this frame, some of usrecently developed a high yield and environmentally advantageous protocol for the fabrication of

conductive graphene-like (GL, Figure 2) layers through a two steps oxidation/reduction method, starting from a nanostructured carbon black (CB).[36] Thanks to the residuals oxygen functional groups on the graphenic layers edges, GL layers feature good stability in water resulting a very versatile nanomaterial and a first candidate for the hybrid materialspreparation.[37]

Here we present the first (at the best of our knowledge) preparation of a eumelanin/GL layers hybrid material (EUmelanin-Graphene Like, EUGL) featuring valuable functional and processing properties, including biocompatibility, easy filmability, high adhesion, electrical conductivity.

The hybrid was characterized by chemical physical, electrical and morphological analyses and its biocompatibility and toxicity wereinvestigated in view of its potential exploitation as bio-interface.

Results and discussion.

Chemical physical characterization. EUGL was characterized integrating analytical and instrumental techniques. The elemental composition (C, N, H) of the EUGL together with those of the pure eumelanin and GL layers are reported in Table 1. The oxygen amount was evaluated by difference. GL layers exhibit a significant amount of oxygen (39.6 wt. %) indicating the presence of oxygen functional groups. The presence of nitrogen is also observed (6.09 wt. %). The COOH amount, evaluated by a fluorimetric test,[38] is $1.7x10^{-7}mol_{COOH}/mg$. The O/C elementratio is 0.56 (comparable to the graphene layers obtained from the reduction of graphite oxide by hydrazine[39]).

Table 1. Samples composition.

Sample	GL wt.%	Elemental composition wt.%			
		C	O	H	N
Eumelanin	0	48.5	36.2	4.0	11.3
GL layers	100	52.9	39.6	1.4	6.1
EUGL	50	54.4 (50.7)	32.3 (37.9)	3.9 (2.7)	9.4 (8.7)

The measured values of C, H and N in the hybrid were compared with a linear combination (1/1 ratio) of measured values for GL layers and eumelanin (see Table 1, brackets). The comparison featured a fair accordance of data, suggesting the actual composition of the hybrid as the outcome of almost quantitative merging of the starting materialsassociated with some oxygen defects likely due to carboxylic groups loss.[40]

Infrared spectroscopy comparison showed in the EUGL spectrum the coexistence of the typical signature of both eumelanin and GL layers (Figure 3) indicating the successfully merging of the two starting materials. Moreover a comparison with the spectrum of the indoles starting mixture confirms the actual formation of eumelanin in presence of GL layers. The broadband feature of the EUGL spectrum is indicative of the π-domains growth, also evidenced by the higherabsorption in the visible region, with respect of neat eumelanin (Figure S1a,b in S.I.).

The most characteristic features of GL layers infrared spectrum are a broad band in the 3000−3700 cm^{-1} range (O−H stretching vibrations due to carboxylic, phenolic groups and possible adsorbed H_2O and, at lower wavenumbers, N−H stretching band due to NH_2 functionalities likely in the form of hydrazones), bands at 1650−1750 cm^{-1} (C=O stretching vibrations from carbonyl and carboxyl groups, anhydrides, lactones, single ketones and quinones) and bands at 1500−1600 cm^{-1} (skeletal vibration of the p-conjugated graphitic domains). Nitrogen atoms in the form of nitro groups were also detected (typical $-NO_2$ stretching vibrations bands at 1560 and 1350 cm^{-1}).

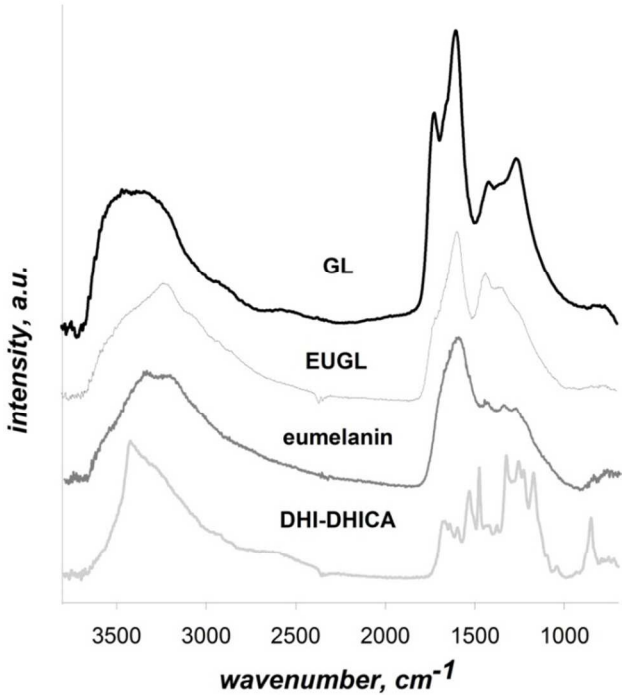

Figure 3. ATR-IR spectra of the parent materials and the hybrid in the 3700-700 cm-1 wavenumber region. Spectra are baseline corrected and shifted.

The EUGL was also investigated by thermogravimetric analysis (TGA) measuring the mass loss of the samples upon heating from room temperature up to 800 °C in oxidative environment(Figure 4).

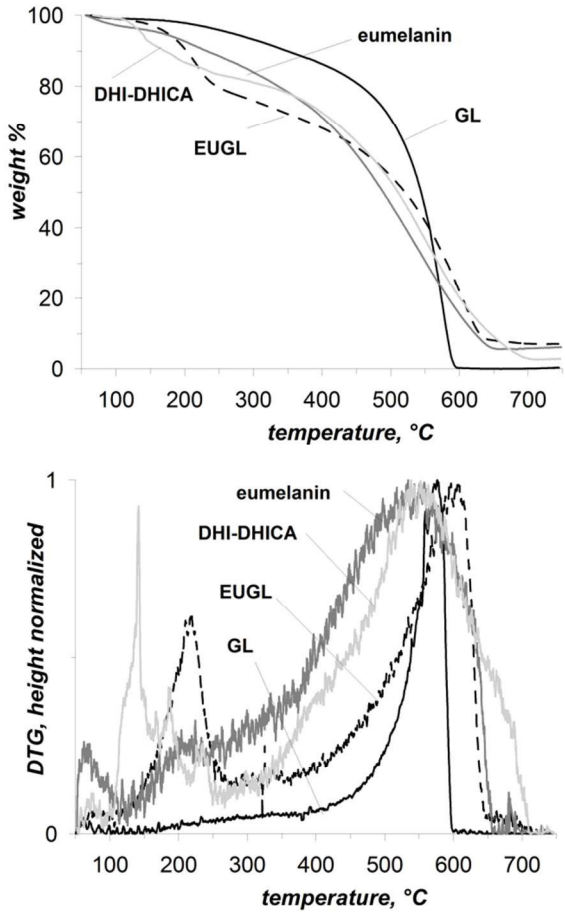

Figure 4. Thermal analyses (TG and DTG) of the parent materials and the hybrid in oxidative environment (air).

TGA curve of GL layers exhibits one main sharp weight loss at 550 °C, corresponding to the bulk oxidation of GL graphitic core. In the case of the TGA curve of both eumelanin and eumelanin precursors a gradual weight loss between 150 and 600 °C is observed, which was likely due to the decomposition of labile oxygen bearing functional groups. A characteristic more pronounced weight loss at 200 °C (20 % weight loss) is also observable for eumelanin. The thermal profile of EUGL exhibits features similar to those of parent materials (weight loss at 200 °C and 550°C, the latter corresponding to the EUGL burnoff). Furthermore,the absence of a sharp weight drop around 550 °C, ~~as~~ observed in the case of neat GL layers, suggests intimate contact between the components of the hybrid(eumelanin and GL layers). Although it is not possible to produce conclusive hypothesis for the eumelanin-GL layers interaction, both covalent bonds and π–π stacking are expected to be involved.Covalent bonds may arise following the attack of nucleophilic units of the GL layers (residual OH and NH_2 groups)[36] toward electrophilic moieties of eumelanin precursors, chiefly quinone and quinonoid systems. π-π stacking is expected on the base of known tendency of graphene related materials to interact with aromatic systems.[4142]

Comparative atomic force microscopy (AFM) inspection of the morphology of eumelanin, GL layers and EUGL thin films indicates a serious modification induced by eumelanin to the GL layers self-assembling and associated adhesion behavior. Indeed, the surface of the neat GL film in Figure 5a looks atomically flat over large areas, with a root mean square (rms) roughness below 1 Å. On the contrary, the eumelanin and the EUGL surfaces exhibit a higher roughness, with different general features. Besides the local roughness, the eumelanin surface (Figure 5b) appears made by macroscopic regions and terraces with different morphology and sharply delimited: the height profile taken along the white line in Figure 5b shows that such surface regions have heights ranging from few to about 10 nm. The hybrid has a locally more granular surface (Figure 5c), resulting in a higher rms roughness compared to the eumelanin one (about 32 nm vs. 10 nm); however, the general character is much more homogenous, exhibiting the same granular aspect over all the sample without sharply defined inhomogeneous regions. It must also be pointed out that the granular feature increases the effective exposed surface of about 15% than its "nominal" area.

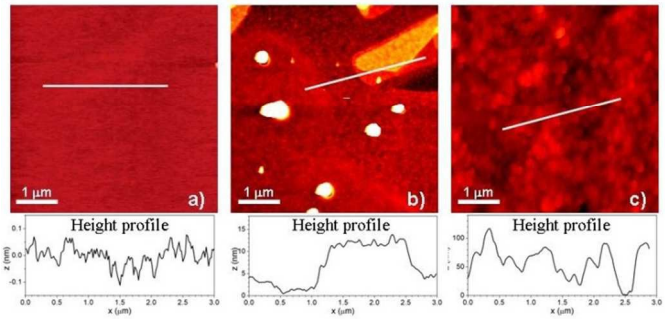

Figure5. AFM: Non-contact AFM images, 5 μm x 5 μm, on: a) GL layers; b) eumelanin; c) EUGL. On each image, a height profile on a line of about 3 μm is also reported, to highlight the surface roughness of each sample. For more detailed images see S.I.Figure S2.

Electrical properties. Electrical characterizations also confirm the actual alteration between properties of EUGL and its parent materials. The measurements of electrical dc resistivity (Figure 6) have been carried out in a standard four contacts geometry for the resistivity evaluation. In Figure6a,b,c, current vs. voltage curves for all the three samples are reported. All the curves show an ohmic behavior, but with extremely different resistance:such strictly linear I-V behavior has already been observed on eumelanin pigments on a wide range of voltage,[43] although some deviations from ohmic behavior were reported at high voltages[44] (nonhomic I-V characteristic and Child's power law at high enough voltage can be a signature of ion transport[45]). A reliable comparison between samples of known thickness is given by the electrical resistivity ρ (or, equivalently, conductivity $\sigma = 1/\rho$), which can be calculated from resistance measurement in the adopted geometry through the van der Pauw algorithm.[46] The thickness measurements have been performed through the AFM: the eumelanin sample was about 100 nm thick, while the GL layers and hybrid films were few microns thick (4 μm and 3 μm respectively). The following resistivity values were estimated:

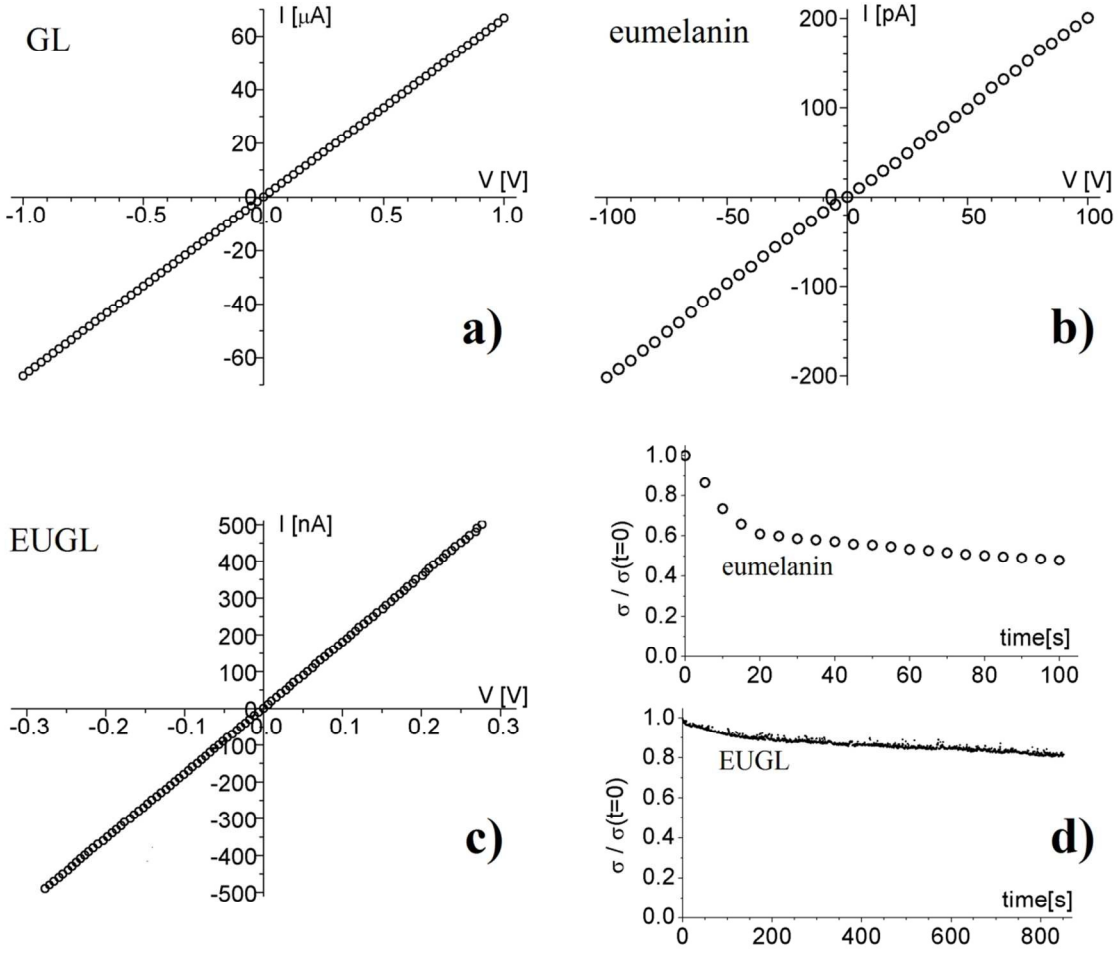

Figure6. I-V curves (in one of the two direction of the van der Pauw configuration) acquired on a) GL layers, b) eumelanin, and c) EUGL samples. d) Time dependent decay of the electrical conductivity on the eumelanin and EUGL films, at fixed voltage (100 V for the eumelanin, 100 mV for the hybrid).

GL, ρ_{GL}= (40 ± 5) Ω·cm (σ_{GL}= (2.5 ± 0.3)·10^3 S/cm);

eumelanin, ρ_{EU}= (2.8 ± 0.4)·10^7Ω·cm (σ_{EU}= (3.6 ± 0.5)·10^{-8} S/cm);

EUGL, ρ_{EUGL}= (1.1 ± 0.2)·10^3Ω·cm (σ_{EUGL}= (9 ± 2)·10^{-4} S/cm).

The high and poor electrical conductivity of GL layers and eumelanin, respectively, are not surprising. In particular, the estimated eumelanin conductivity is about at the middle of the wide range of measured values for eumelanin samples[15,36] (eight orders of magnitudes, since electrical transport in eumelanin is strongly affected by some extrinsic factors such as humidity or photodoping).

On the other hand EUGL exhibits an electrical conductivity more than four orders of magnitudes greater than the one of parent eumelanin. Another interesting finding is the observation of a time-decay of electrical conductivity in the eumelanin and hybrid samples (while this phenomenon is absent in the GL film). As shown in Figure6d, the decay of σ takes place, on the two samples, on very different time scales and in very different amount, being much faster and pronounced in the eumelanin than in the hybrid compound. On the other hand, a common feature is the presence of two different time-scales in the decay curves: both curves exhibit a "fast" initial decay, followed by a further slower decrease. The transition between the two regimes takes place after less than 20s (and at about 60% of the initial conductivity) in eumelanin, and after a time about 10 times larger (at about 90% of its initial conductivity) in the hybrid material.

This result is in qualitative agreement with what recently observed on similar eumelanin samples[14] and somehow similar to results reported on other (eu)melanin samples[47]. The fast initial decay can be probably ascribed to the ionic current that can flow in the eumelanin or in the hybrid, but it is blocked at the silver electrodes designed for the measurements. More precisely, weakly bonded protons (H^+) in the interspaces of the stacked structure of our compounds can be driven by the applied electric field, producing the ionic current in the measured sample. However, such current flow cannot take place in the conventional metal constituiting the electrodes, and protons are therefore blocked at the interface between the samples and the electrodes. The resulting counter-field is responsible of the observed initial decay of the electrical conductivity vs. time.After this transient, the only electronic contribution survives, but it also experiences a slower time decay, which is probably driven by trapping phenomena occurring in such disordered samples. Therefore, the σ decay and its double time-scale suggest the presence of a double contribution (ionic and electronic) to the electrical transport in both eumelanin and hybrid samples. On the contrary, in the GL film we did not observe any decrease of the electrical conductivity vs. time: thisdoes not necessarily mean that a proton transport is missing, but, if present, it is completely overruled by electron conductivity. The stronger incidence of the initial fast decay in the eumelanin seems to indicate that in this sample the ionic contribution is much more important (relatively to the electronic one) than in the hybrid compound: in the latter, therefore, the conjunction with the GL layers adds electronic carriers that are likely responsible of the improved electrical conductivity.

Impedance spectroscopy measurements between 10 Hz and 100 kHz are reported in Figure 7a, b, c for the GL layers, eumelanin and EUGL samples respectively. In this frequency range, the experimental data are well fitted by a common equivalent Randless circuit, schematically reported in Figure 7d. In this model, CPE is a constant phase element, whose complex impedance vs. angular frequency ω can be written as $Z_{CPE} = 1/(j\omega)^m Q$: j is the imaginary unit, Q and m (with $0 \le m \le 1$) are fitting parameter (for m = 0 the CPE acts as a pure resistor of value Q^{-1}; for m = 1, it acts as a pure capacitor Q). Z_W is the impedance of a Warburg element: $Z_W = A_W/(j\omega)^{1/2}$. The Randless scheme is phenomenologically introduced to describe the ac transport in many complex organic compounds: Z_{CPE} includes the effects of a double layer capacitance and a surface modification capacitance, while the Warburg elements describes the diffusion to the electrode surface. In our case, the use of the Randless circuit is suggested by the data on EUGL, whose Nyquist plot (inset of Figure 7c) exhibits the typical features produced by this model: a "smashed" semi-circle as a consequence of the non-ideal capacitance of the CPE, and an upward nearly-linear arm due to the role of the Warburg element at low frequencies. It is worth to note, from Figure 7b (and its inset) that the data on eumelanin do not show these strong signs: we decided however to do not change the fitting model to avoid to introduce further degrees of freedom and to allow a direct comparison between the results on both samples. The fit procedure gives for the eumelanin sample m = 0.99: the CPE basically acts a pure capacitor. We estimate a specific capacitance of about 1 μF/cm^2, which, however, is likely an underestimation of the

intrinsic specific capacitance of the material (due to the poor grain connection). As a comparison, we get m = 0.88 on EUGL, and a pronounced role of the Warburg impedance already in the explored frequency range (on the eumelanin, the fit curve is quite non-sensitive to the Warburg arm of the circuit: lower frequencies need to be explored to understand the role of this element). This difference can be an indication of a relevant forward-backward jumps of the ions in the ac transport;[48] however, this result could be also a consequence of a worst connection between different large regions of the eumelanin films than between grains in the EUGL hybrid sample. As concerns the GL layers, the Randless circuit must also be invoked to get a satisfying fit, as already observed on reduced graphene oxide.[49]

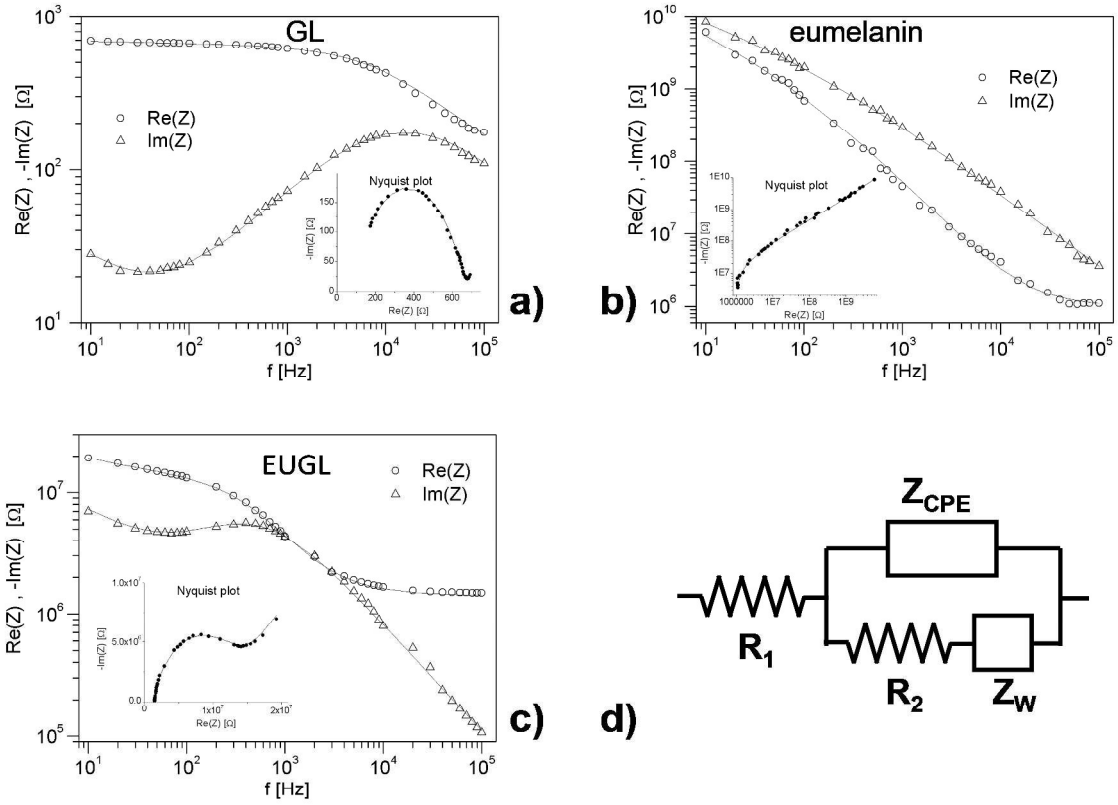

Figure 7. Impedance spectroscopy measurements on a) GL layers, b) eumelanin, and c) EUGL, plotted as real and imaginary part vs. frequency. In the insets: Nyquist plot per each set of measurements. Each plot reports both experimental data (scatter) and the theoretical fit (continuous line). d) The Randless circuit used for modeling the experimental impedance curves.

Mammalian cell biocompatibility. Biocompatibility of EUGL was checked in mammalian cell cultures in vitro. In order to screen a ran ge of different cellular requirements two different cell typologies we re chosen: the Murine Embryonic Stem Cell (ESC) and Rat Microgli al Cell (MC). ESC is a cell population of particular interest for tissue engineering application and it is under scrutiny for compatibility wit h classical electro-active materials[50]. The MCs are a cell population belonging to the class of neuroglial cells, that plays an active role in t he central nervous system (CNS) function/homeostasis and is highly sensitive to electrical stimuli. They are the primary cells that are acti vated in response to inflammatory stimulation[51] an thus they are of p articular relevance in the investigation of the toxic/proinflammatory potential of an electroconductive substrate.

Few previous papers have appeared in the field, one reporting the abi lity of thin films from commercial eumelanin to enhance Schwann ce ll growth and neurite extension films growth,[23] and a study on this sp ecific ESCs disclosing the biocompatibility of AISSP fabricated eum elanin thin film[30].

In a series of experiments we addressed the survival and proliferatio n of undifferentiated ESCs grown on EUGLfilms and the preservatio n of ESC morphology. Before cell seeding EUGL film stability to cu lture media was checked. Even after extensive sonication treatment i n buffer the films remained stable and no detectable release of GL la yers as well as eumelanin was observed.

To assess the ability of EUGL films to support the survival of ESCs, undifferentiated ESCs were trypsinized into a single-cell suspension and 6×10^4 cells/cm^2 were plated on 100 mm EUGL-coated dish in E SC medium. The medium was changed every day for two days. As s hown in Figure 8 EUGL coating supported adhesion and colony for mation of ESCs. ESCs proliferation was evaluated by counting cells after trypsinization and dissociation at 2 days in colonies plated on di shes coated with EUGL or with gelatin (as control).

As reported in Figure S3of S.I.the growth curves of ESCs plated on EUGL showed a trend comparable with the same cells plated on gela tin indicating that EUGL does support ESCs proliferation.

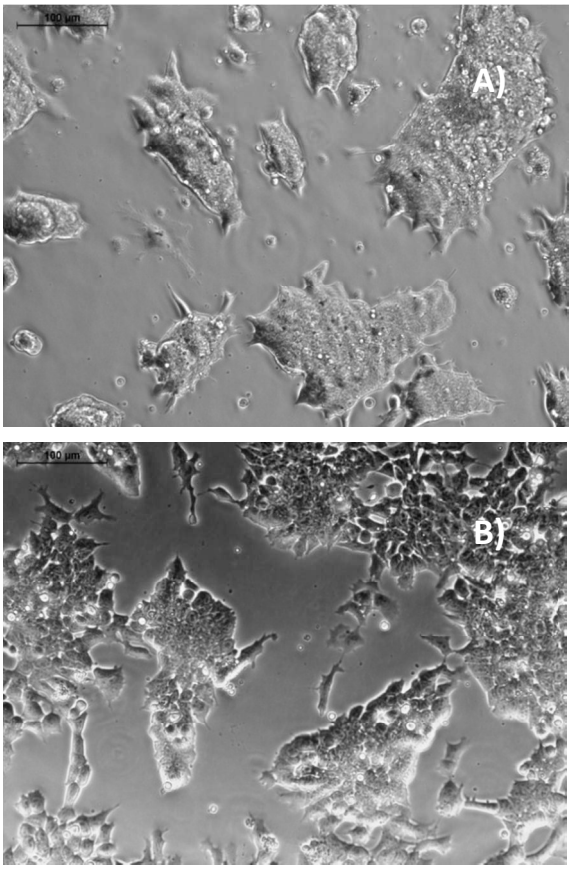

Figure 8. Phase contrast image of ESC colonies two days after seedi ng on dishes coated with EUGL or gelatin. Stem cells grown on EU GL film (upper image: A) and on a Petri gelatin-coated plate as a co ntrol (lower image: B). Scale bars: 100µm

In a separate experiment the level of the apoptosis hallmark active caspase-3 was analyzed in order to check the absence of abnormal cell death in healthy colonies and highlighted by the morphological analysis. As shown in Figure S4of SI, western blot analysis revealed that there is no accumulation of cleaved caspase-3 to the detriment of the uncleaved one that is normally present in healthy cells.

The in vitro viability of MC cultures over EUGL films was tested by different approaches: checking the release from damaged cells of the cytosolic enzyme lactate dehydrogenase (LDH)[52] by using a LDH diagnostic kit; and the possible effect on the cell mitochondrial function by the MTT test [3-(4,5-dimethylthiazol-2-yl)-2,5-diphenyltetrazolium bromide (MTT)][53].

The measure of LDH in the cell culture supernatants after 24h indicated no significant increase of LDH levels in supernatants of cells grown on EUGL indicative of a negligible cytotoxicity of these substrates on microglia cells. Interestingly, the levels of LDH in cell

culture supernatants of cells grown on eumelanin substrates were significantly increased (Figure 9) showing a cytotoxic potential of this substrate on microglial cells. The MTT test further confirmed microglia cell viability over EUGL.

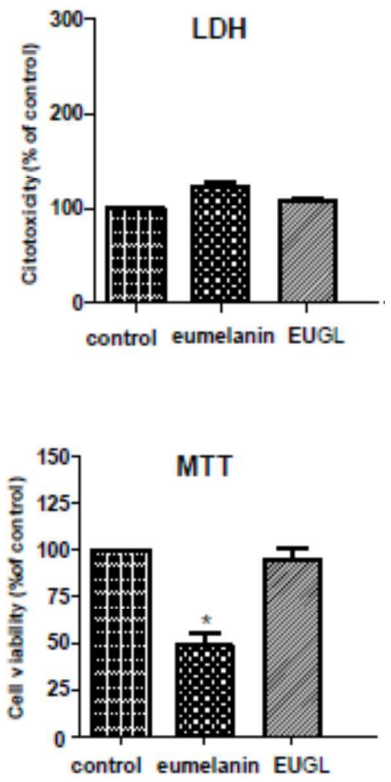

Figure 9. Effects of melanin and EUGL hybrid on microglial cell membrane integrity (LDH) and on microglial cell mitochondrial membrane function (MTT). Primary rat microglial cells were grown on eumelanin and EUGL for 24h. The cytotoxicity was assessed respectively by lactate dehydrogenase (LDH) assays and by MTT reduction assay. Values are expressed as mean ± S.D (n=4).

In a further series of experiments the analysis of NO production by microglia cells seeded on EUGL was addressed showing that no inflammatory potential could be ascribed to the EUGL substrate confirming the actual MC viability when cultured in vitro over the EUGL (Figure S5 of SI).

Overall, these data disclose a wide biocompatibility of EUGL resulting not toxic for ESCs and MCs and bereft of pro-inflammatory potential on microglial cells. It is interesting to observe here that, differently from EUGL films, eumelanin films do not only affect significantly the viability of microglial cells but possess a remarkable pro-inflammatory potential towards these cells. This could be due to the phagocytic nature of microglia cells, a cell typology of hematopoietic origin. Indeed it could be speculated that the different morphology and chemical nature of EUGL and eumelanin could have stimulated, in the latter case, phagocytic activity in these cells and, therefore, induced cell death. However, this hypothesis deserves further investigations, in particular in relation with the morphology of EUGL vs that of eumelanin.

Given the poor adhesivity of GL film on substrates the intrinsic biocompatibility and toxicity toward mammalian cells of neat GL layers cannot be evaluated under the same experimental conditions reported for EUGL.

Experimental

Materials. All commercially available reagents were used as received and all the solvents were analytical grade quality. 5,6-Dihydroxindole (DHI) and 2-carboxy- 5,6-Dihydroxindole (DHICA) were prepared according to a reported procedure[54]. CB N110 type (furnace CB) was obtained by Sid Richardson Carbon Co. CB is a monodispersion of chain-like aggregates of spherical primary particles with average diameters of 15-20 nm. The hydrodynamic diameter of the aggregates is 170 ± 10 nm and the surface area is 139 $m^2 g^{-1}$ (BET method).

Details about the preparation of GL layers, DHI and DHICA are reported in S.I. section.

EUGL preparation. GL aqueous suspension (1 mg/mL) was added to the DHI-DHICA 3:1 mixture dissolved in methanol by ultrasonic agitation (20 mg/mL). The suspension was kept for 10 min under agitation with a magnetic stirrer afterwards pH was adjusted to 8 by the addition of ammonia solution (28% in water) allowing indole autoxidation and polymerization. After 1 h the reaction was quenched by adding acetic acid (1 M) until pH 4 was established. A EUGL film was obtained by drop casting the suspension onto clean substrates (well plates for biological essays, quartz and mica plates). For bulk analyses the suspension was dried in oven at 80 °C. After drying the hybrid resulted insoluble in water.

Details about the analytical techniques used to characterized the materials and about the in vitro tests are reported in S.I. section.

Conclusions

In light of possible effective interfacing of two π-materials, namely eumelanin and GL layers, we speculated on the possibility to access

a biocompatible substrate featuring eumelanin typical properties, including adhesion and water stability, but exhibiting improved electrical conductivity with respect to the natural pigment.

In situ eumelanin preparation allowed to entrap GL layers producing a hybrid material possessing promising properties in view of application in bioelectronics.

A possible model representation of the EUGL structure is reported in Figure 10 depicting EUGL as eumelanin coated GL layers. This hypothesis arises from the know properties of eumelanin, chiefly adhesion and affinity toward aromatic systems,[1855] and the observed adhesivity, mechanical stability to water and biocompatibility of EUGL. Indeed, given the water solubility of GL layers,[36] such EUGL features are ascribable to external exposition of eumelanin.

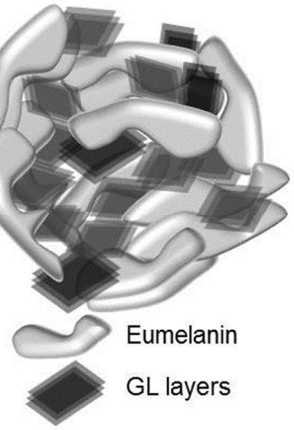

Figure 10. Hypothesized morphologies of EUGL.

The wide biocompatibility of EUGL, capable to allow ESC and MC culture, pairs with an unprecedented conductivity in a eumelanin derivative. EUGL exhibits an electrical conductivity more than 4 orders of magnitudes greater than the one of parent eumelanin compound. It may be speculated that this conductivity increment with respect to eumelanin, besides the chemical nature of the EUGL, it has a contribution from the improved large scale homogeneity of the samples. This hypothesis would be supported by AFM images and associated to a better connection between uniformly distributed grains. In addition, a role of possible percolating paths of GL layers inside the compounds cannot be excluded (even if unlikely), and represents an issue deserving further investigation.

The properties of the EUGL films described herein may expand the scope of eumelanin in bioelectronics paving the way to true biocompatible organic electrochemical transistor-like[56, 57]interfaces capable of translating cellular activity in electrical signals.

Acknowledgements

This work was supported by a grant from Italian MIUR (PRIN 2010-2011, 010PFLRJR "PROxi" project), by a grant to SP from Ministry of University and Research for the projects: Futuro in Ricerca 2013 (RBFR13YZ2Y) and was carried out in the frame of the EuMelaNet program (http://www.espcr.org/eumelanet) and the PolyMed project within the FP7-PEOPLE-2013-IRSES frame, PIRSES-GA-2013-612538. The authorsacknowledgethe Accordo CNR-MSE "Utilizzo pulito dei combustibili fossili ai fini del risparmio energetico" 2011-2012 for the financialsupport.

Notes and references

[a]Istituto di Ricerche sulla Combustione (IRC) - CNR, P.leTecchio 80, I-80125 Naples – Italy
[b]Dipartimento di Fisica, Università di Napoli Federico II via Cintia, I-80126, Naples, Italy
[c]CNR-SPIN via Cintia, Naples 80125, Italy
[d]Department of Clinical Medicine, University La Sapienza, Rome, Italy; Inst. of Traslational Pharmacology, National Research Council (CNR), Rome, Italy
[e]Department of Physiology and Pharmacology, University La Sapienza, Rome, Italy
[f] Department of Molecular Medicine and Medical Biotechnology, University of Naples "Federico II"
[g]CeingeBiotecnologieAvanzate Via Gaetano Salvatore 486, 80145 Naples, Italy
[h] Department of Chemical Sciences, University of Naples "Federico II" Via Cintia 4, I-80126 Naples, Italy E-mail: alessandro.pezzella@unina.it

† Electronic Supplementary Information (ESI) available: [details of any supplementary information available should be included here]. See DOI: 10.1039/b000000x/

1. J. Rivnay, R. M. Owens and G. G. Malliaras, *Chem Mater*, 2014, **26**, 679-685.
2. M. Berggren and A. Richter-Dahlfors, *Adv Mater*, 2007, **19**, 3201-3213.
3. M. d'Ischia, A. Napolitano, A. Pezzella, P. Meredith and T. Sarna, *Angew Chem Int Edit*, 2009, **48**, 3914-3921.
4. P. Meredith, C. J. Bettinger, M. Irimia-Vladu, A. B. Mostert and P. E. Schwenn, *Rep Prog Phys*, 2013, **76**, 034501.
5. M. d'Ischia, K. Wakamatsu, A. Napolitano, S. Briganti, J. C. Garcia-Borron, D. Kovacs, P. Meredith, A. Pezzella, M. Picardo, T. Sarna, J. D. Simon and S. Ito, *PigmCell Melanoma R*, 2013, **26**, 616-633.
6. C. Santato and F. Cicoira, *Organic Electronics Emerging Concepts and Technologies Preface*, Blackwell Science Publ, Oxford, 2013.
7. S. Ito, *PigmCell Melanoma R*, 2009, **22**, 12-13.
8. S. Ito, *Melanins and Melanosomes: Biosynthesis, Biogenesis, Physiological, and Pathological Functions*, Wiley-V C H Verlag Gmbh, Pappelallee 3, W-69469 Weinheim, Germany, 2011.
9. L. Ascione, A. Pezzella, V. Ambrogi, C. Carfagna and M. d'Ischia, *Photochem photobiol*, 2013, **89**, 314-318.

10. A. Pezzella, A. Iadonisi, S. Valerio, L. Panzella, A. Napolitano, M. Adinolfi and M. D'Ischia, *J Am Chem Soc*, 2009, **131**, 15270-15275.
11. A. Huijser, A. Pezzella and V. Sundstrom, *Phys chem chem phys*, 2011, **13**, 9119-9127.
12. V. Capozzi, G. Perna, P. Carmone, A. Gallone, M. Lastella, E. Mezzenga, G. Quartucci, M. Ambrico, V. Augelli, P. F. Biagi, T. Ligonzo, A. Minafra, L. Schiavulli, M. Pallara and R. Cicero, *Thin Solid Films*, 2006, **511**, 362-366.
13. D. Rettenwander, P. Blaha, R. Laskowski, K. Schwarz, P. Bottke, M. Wilkening, C. A. Geiger and G. Amthauer, *Chem Mater*, 2014, **26**, 2617-2623.
14. J. Wünsche, Y. Deng, P. Kumar, E. Di Mauro, E. Josberger, J. Sayago, A. Pezzella, F. Soavi, F. Cicoira, M. Rolandi and C. Santato, *Chem Mater*, 2015, **27**, 436-442.
15. P. Meredith and T. Sarna, *Pigm cell res*, 2006, **19**, 572-594.
16. Y. Liu and J. D. Simon, *Pigm cell res*, 2005, **18**, 42-48.
17. S. Reale, M. Crucianelli, A. Pezzella, M. D'Ischia and F. De Angelis, *J Mass Spectrom*, 2012, **47**, 49-53.
18. M. Arzillo, G. Mangiapia, A. Pezzella, R. K. Heenan, A. Radulescu, L. Paduano and M. D'Ischia, *Biomacromolecules*, 2012, **13**, 2379-2390.
19. D. Kai, M. P. Prabhakaran, G. R. Jin and S. Ramakrishna, *J Mater Chem B*, 2013, **1**, 2305-2314.
20. Q. L. Fan, K. Cheng, X. Hu, X. W. Ma, R. P. Zhang, M. Yang, X. M. Lu, L. Xing, W. Huang, S. S. Gambhir and Z. Cheng, *J Am Chem Soc*, 2014, **136**, 15185-15194.
21. A. Pezzella, M. Barra, A. Musto, A. Navarra, M. Alfe, P. Manini, S. Parisi, A. Cassinese, V. Criscuolo and M. d'Ischia, *Mater Horiz*, 2015, **2**, 212-220.
22. M. Muskovich and C. J. Bettinger, *Adv Healthc Mater*, 2012, **1**, 248-266.
23. C. J. Bettinger, P. P. Bruggeman, A. Misra, J. T. Borenstein and R. Langer, *Biomaterials*, 2009, **30**, 3050-3057.
24. C. Kremer, C. Witte, S. L. Neale, J. Reboud, M. P. Barrett and J. M. Cooper, *Angew Chem Int Edit*, 2014, **53**, 842-846.
25. L. Y. Feng, L. Wu and X. G. Qu, *Adv Mater*, 2013, **25**, 168-186.
26. J. Wunsche, F. Cicoira, C. F. O. Graeff and C. Santato, *J Mater Chem B*, 2013, **1**, 3836-3842.
27. J. Wunsche, L. Cardenas, F. Rosei, F. Cicoira, R. Gauvin, C. F. O. Graeff, S. Poulin, A. Pezzella and C. Santato, *Adv Funct Mater*, 2013, **23**, 5591-5598.
28. F. Bloisi, A. Pezzella, M. Barra, F. Chiarella, A. Cassinese and L. Vicari, *J Appl Phys*, 2011, **110**.
29. F. Bloisi, A. Pezzella, M. Barra, M. Alfe, F. Chiarella, A. Cassinese and L. Vicari, *Appl Phys a-Mater*, 2011, **105**, 619-627.
30. C. Pezzella, L. Guarino and A. Piscitelli, *Cell mol life sci*, 2015, **72**, 923-940.
31. X. W. Ou, P. L. Chen, L. Jiang, Y. F. Shen, W. P. Hu and M. H. Liu, *Adv Funct Mater*, 2014, **24**, 543-554.
32. H. A. Becerril, R. M. Stoltenberg, M. L. Tang, M. E. Roberts, Z. F. Liu, Y. S. Chen, D. H. Kim, B. L. Lee, S. Lee and Z. A. Bao, *Acs Nano*, 2010, **4**, 6343-6352.
33. J. B. Wu, M. Agrawal, H. A. Becerril, Z. N. Bao, Z. F. Liu, Y. S. Chen and P. Peumans, *Acs Nano*, 2010, **4**, 43-48.
34. J. Kim, L. J. Cote and J. X. Huang, *Accounts Chem Res*, 2012, **45**, 1356-1364.
35. X. Wang, L. J. Zhi and K. Mullen, *Nano Lett*, 2008, **8**, 323-327.
36. M. Alfe, V. Gargiulo, R. Di Capua, F. Chiarella, J. N. Rouzaud, A. Vergara and A. Ciajolo, *Acs Appl Mater Inter*, 2012, **4**, 4491-4498.
37. M. Alfe, V. Gargiulo, L. Lisi and R. Di Capua, *Mater Chem Phys*, 2014, **147**, 744-750.
38. S. Visentin, N. Barbero, S. Musso, V. Mussi, C. Biale, R. Ploeger and G. Viscardi, *Chem Commun*, 2010, **46**, 1443-1445.
39. S. Stankovich, R. D. Piner, S. T. Nguyen and R. S. Ruoff, *Carbon*, 2006, **44**, 3342-3347.
40. M. D'Ischia, K. Wakamatsu, A. Napolitano, S. Briganti, J. C. Garcia-Borron, D. Kovacs, P. Meredith, A. Pezzella, M. Picardo, T. Sarna, J. D. Simon and S. Ito, *Pigm Cell Melanoma R*, 2013, **26**, 616-633.
41. F. Zhang, X. Chen, R. A. Boulos, F. Md Yasin, H. Lu, C. Raston and H. Zhang, *Chem Commun*, 2013, **49**, 4845-4847.
42. F. De Marchi, D. Cui, J. Lipton-Duffin, C. Santato, J. M. MacLeod and F. Rosei, *J Chem Phys*, 2015, **142**.
43. M. M. Jastrzebska, H. Isotalo, J. Paloheimo and H. Stubb, *J Biomat Sci-Polym E*, 1995, **7**, 577-586.
44. W. Osak, K. Tkacz, J. Slawinski and H. Czternastek, *Biopolymers*, 1989, **28**, 1875-1883.
45. L. Glasser and R. L. Fiederlein, *Am j clin pathol*, 1979, **72**, 956-962.
46. L. J. van der Pauw, *Philips Res Rep*, 1973, **28**, 158-178.
47. S. R. Cicco, M. Ambrico, P. F. Ambrico, M. M. Talamo, A. Cardone, T. Ligonzo, R. Di Mundo, C. Giannini, T. Sibillano, G. M. Farinola, P. Manini, A. Napolitano, V. Criscuolo and M. D'Ischia, *J Mater Chem C*, 2015, **3**, 2810-2816.
48. M. R. S. Abouzari, F. Berkemeier, G. Schmitz and D. Wilmer, *Solid State Ionincs*, 2009, **180**, 922-927.
49. E. Casero, A. M. Parra-Alfambra, M. D. Petit-Dominguez, F. Pariente, E. Lorenzo and C. Alonso, *ElectrochemCommun*, 2012, **20**, 63-66.
50. I. N. Wang, J. T. Robinson, G. Do, G. Hong, D. R. Gould, H. Dai and P. C. Yang, *Small*, 2014, **10**, 1479-1484.
51. M. L. Block, L. Zecca and J. S. Hong, *Nat rev Neurosci*, 2007, **8**, 57-69.
52. S. M. Hussain and J. M. Frazier, *Toxicol sci*, 2002, **69**, 424-432.
53. J. Carmichael, W. G. DeGraff, A. F. Gazdar, J. D. Minna and J. B. Mitchell, *Cancer res*, 1987, **47**, 943-946.
54. R. Edge, M. D'Ischia, E. J. Land, A. Napolitano, S. Navaratnam, L. Panzella, A. Pezzella, C. A. Ramsden and P. A. Riley, *Pigm Cell Res*, 2006, **19**, 443-450.
55. T. Sarna and H. A. Swartz, in *The Pigmentary System: Physiology and Pathophysiology: Second Edition*, 2007, pp. 311-341.
56. M. Bongo, O. Winther-Jensen, S. Himmelberger, X. Strakosas, M. Ramuz, A. Hama, E. Stavrinidou, G. G. Malliaras, A. Salleo, B. Winther-Jensen and R. M. Owens, *J Mater Chem B*, 2013, **1**, 3860-3867.
57. D. Khodagholy, J. Rivnay, M. Sessolo, M. Gurfinkel, P. Leleux, L. H. Jimison, E. Stavrinidou, T. Herve, S. Sanaur, R. M. Owens and G. G. Malliaras, *Nat Commun*, 2013, **4**.

TOC